DEVELOPMENT OF A POWER CONTROL ALGORITHM BASED ON THROUGHPUT WINDOW FOR WIRELESS BODY AREA NETWORKS

Tien Anh Bui[1], Thanh Quan Do[2,*], Quang Quan Phung[3], Thanh Hiep Pham[1]

[1]*Faculty of Radio-Electronic Engineering, Le Quy Don Technical University*
[2]*Faculty of Technical Management, Le Quy Don Technical University*
[3]*Vietnam-Japan International Cooperation Center for Science and Technology, Le Quy Don Technical University*

Abstract

Sensors in Wireless Body Area Networks (WBANs) require low power consumption to ensure continuous long-term operation while maintaining accurate and stable data transmission. This article proposes a novel power control algorithm that significantly improves energy efficiency for WBAN sensors compared to existing schemes. The proposed "Throughput Window-based Power Control" (TWC) algorithm ensures that the sensor's throughput remains within a predefined range, aligning with system requirements. Simulation results demonstrate that TWC not only significantly reduces energy consumption but also maintains stable communication performance with high reliability under the unique transmission conditions of WBANs. In particular, TWC achieves the highest average energy efficiency, which is 1.5 times higher than the Max-Min Power Control (MMC) algorithm and 7.5 times higher than the No Power Control (NPC) scenario. Moreover, TWC yields the lowest average power consumption, reaching 0.75 times that of MMC and only 0.3 times that of NPC. Compared to MMC and NPC, TWC offers superior energy-saving capability while ensuring quality of service. These findings support the development of energy-autonomous WBAN models that meet the requirements of advanced health monitoring applications.

Keywords: *Wireless body area networks; power control; energy efficiency; communication performance.*

1. Introduction

Wireless Body Area Networks (WBANs) play a crucial role in monitoring and tracking human physiological parameters [1], [2]. WBAN sensors, which are either attached to the body surface or implanted, are responsible for measuring vital signs such as heart rate, temperature, blood pressure, and activity levels. These networks facilitate

[*] Corresponding author, email: dtquan@lqdtu.edu.vn
DOI: 10.56651/lqdtu.jst.v20.n02.950

health monitoring, enable early detection of abnormalities, and enhance medical care efficiency. However, WBAN sensors typically operate in highly dynamic signal environments and are constrained by limited energy resources, posing challenges in maintaining system performance and reliability. Therefore, optimizing energy consumption to extend sensor lifespan is a critical requirement in medical and healthcare applications [3], [4]. Several studies have focused on developing power control methods aimed at not only reducing energy consumption but also optimizing overall communication performance.

One of the representative approaches is the cooperative power control algorithm proposed in [5] which aims to mitigate interference in WBANs using two-hop communication by optimizing relay node selection based on the signal-to-noise-plus-interference ratio and transmission power. However, this method involves complex computations for relay node selection and may increase energy consumption due to the additional relay communication overhead. Meanwhile, the study in [6] applies adaptive power control based on kinematic and physiological data to predict channel conditions and optimize transmission power. However, this approach requires extensive data processing, making it unsuitable for resource-constrained sensors and potentially leading to higher energy consumption, thereby affecting battery lifespan.

Additionally, the study in [7] proposes an energy-saving method for health monitoring by leveraging edge computing. Specifically, data is processed directly at edge sensors to filter out non-essential information, while an anomaly detection model is deployed at the edge device to minimize the amount of data transmitted to the central server. However, this approach may result in the loss of critical data if the filtering threshold is not appropriately set, and its effectiveness depends on the accuracy of the anomaly detection model at the edge.

Furthermore, the study in [8] proposes an adaptive power control algorithm based on the received signal strength indicator, allowing sensors to adjust their power based on feedback from the access point (AP). However, this method is not optimal when the body is in motion, as it does not effectively mitigate multipath interference and fading. Additionally, it relies on feedback from the AP which may lead to instability when the communication channel fluctuates. Meanwhile, the study in [9] employs reinforcement learning to simultaneously optimize power and transmission time, thereby enhancing WBAN performance. Although promising, reinforcement learning requires a long

training period and may not be responsive enough when the number of sensors dynamically changes. Another approach to improving sensor throughput in WBANs is the multi-connectivity WBAN model combined with the MMC algorithm, as proposed in [10]. However, the MMC algorithm does not address the issue of energy efficiency.

Overall, existing studies have proposed various power control methods to enhance transmission performance in WBANs. However, most approaches still face challenges in balancing energy efficiency and link reliability. Therefore, a more flexible and adaptive solution is required to maintain stable connectivity while improving energy efficiency in WBANs. To address this challenge, this article proposes the TWC algorithm. The TWC algorithm not only enhances communication performance but also conserves energy by adjusting sensor power based on throughput requirements, thereby extending the lifespan of WBAN devices. The core mechanism of TWC involves regulating transmission power within a predefined throughput window, ensuring link quality while improving energy efficiency. Compared to [6], which relies on biosignals and kinematic data for adaptive power control, the proposed TWC algorithm eliminates the need for extensive sensor fusion and processing. While [6] is suitable for flexible applications, its dependency on motion-related data may limit its effectiveness in maintaining consistent throughput under varying channel conditions. In contrast to [9], which uses deep reinforcement learning to jointly optimize power and time allocation, TWC adopts a simpler control structure that avoids high computational overhead and long convergence times. This makes TWC more practical for real-time applications on energy-constrained WBAN sensors. This study aims to develop a more efficient solution for WBANs, contributing to improved health monitoring with high energy efficiency.

2. System model

2.1. System architecture

The multi-connectivity WBAN model, illustrated in Fig. 1, consists of multiple patients equipped with sensors that communicate with wall-mounted APs in a hospital treatment room. On each patient's body, sensors are placed at various locations such as the chest, abdomen, legs, and arms. Each sensor is equipped with a single antenna and is responsible for collecting and transmitting physiological data in real time. The total number of sensors in the system is denoted as K. On each patient's body, sensors are placed at various locations such as the chest, abdomen, legs, and arms. Each sensor is equipped with a single antenna and is responsible for collecting and transmitting

physiological data in real time. The total number of sensors in the system is denoted as *K*. The APs are installed at a standard height of 2.5 meters on the wall to optimize signal reception from all sensors in the room. This placement ensures stable and uniform connectivity throughout the monitoring space. The total number of APs in the system is denoted as *M*, with each AP equipped with a single antenna to facilitate efficient data transmission and reception. The primary function of the APs is to collect signals transmitted from the sensors and relay the data to the central processing unit (CPU) via a high-speed wired connection for analysis and processing. This process provides detailed insights into the user's physiological condition, supporting diagnostics and enabling timely medical decision-making.

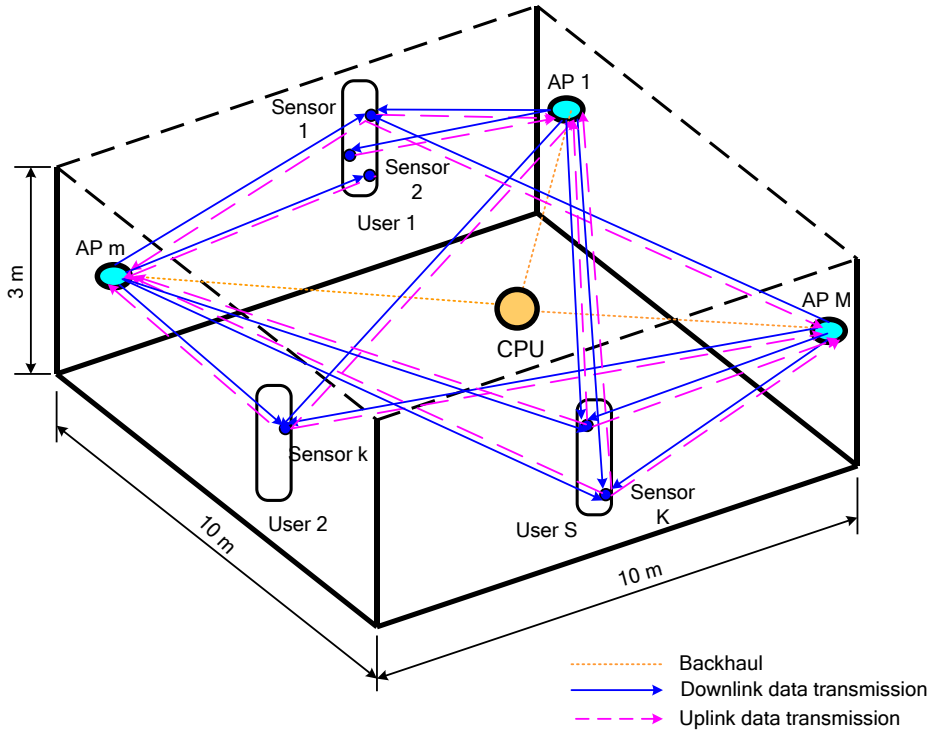

Fig. 1. Multi-connectivity WBAN system model.

2.2. Data transmission method

WBAN applications primarily require uplink data transmission from sensors to APs to ensure the accurate delivery of critical parameters such as electrocardiogram (ECG), electroencephalogram (EEG), blood oxygen levels, and activity monitoring in real time. This enables the early detection of abnormal conditions and timely medical intervention. Therefore, this article focuses on uplink power control to optimize sensor energy

consumption, thereby extending device lifespan and ensuring the sustainable operation of the multi-connectivity WBAN model.

Let g_{mk} denotes the channel coefficient between the m^{th} AP and the s^{th} sensor. The channel is modeled as:

$$g_{mk} = \sqrt{\beta_{mk}} h_{mk}, \quad (1)$$

where h_{mk} captures the small-scale fading component, typically modeled as a complex Gaussian random variable, and β_{mk} represents the large-scale fading which accounts for path loss and shadowing effects.

2.3. Uplink traning

Let τ^c denotes the coherence interval length, expressed in samples, which is calculated as the product of the coherence time and the coherence bandwidth. Within each coherence interval, a duration of τ^{cf} samples is allocated for uplink pilot transmission. To guarantee reliable channel estimation, the training duration τtrττtr must satisfy the condition $\tau^{cf} < \tau^c$. During this uplink training phase, all K sensors simultaneously transmit their individual pilot signals, each comprising τ^{cf} samples, to the APs. The pilot sequence assigned to the ssth sensor is defined as $\sqrt{\tau^{cf}}\boldsymbol{\varphi}_k \in \mathbb{C}^{\tau^{cf}\times 1}$, where $\boldsymbol{\varphi}_k$ is a unit-norm vector satisfying $\|\boldsymbol{\varphi}_k\|^2 = 1$ for k = 1,..., K. As a result, the m^{th} AP receives a pilot observation vector of size $\tau^{cf} \times 1$ which can be expressed as:

$$\mathbf{y}_{\mathrm{p},m} = \sqrt{\tau^{cf}\rho_p}\sum_{k=1}^{K} g_{mk}\boldsymbol{\varphi}_k + \mathbf{w}_{\mathrm{p},m}, \quad (2)$$

where ρ_p denotes the normalized signal-to-noise ratio (SNR) corresponding to each pilot symbol. The noise vector at the m^{th} AP is denoted by $\mathbf{w}_{\mathrm{p},m}$ whose entries are assumed to be independent and identically distributed complex Gaussian random variables with distribution. Given the received pilot signal $\mathbf{y}_{\mathrm{p},m}$, the m^{th} AP proceeds to estimate the wireless channel g_{mk} for each sensor k = 1, 2,…, K. To facilitate this, let $\breve{\mathrm{y}}_{\mathrm{p},mk}$ represent the projection of the received pilot signal $\mathbf{y}_{\mathrm{p},m}$ onto the conjugate transpose of the pilot sequence $\boldsymbol{\varphi}_k^H$.

$$\breve{\mathrm{y}}_{\mathrm{p},mk} = \boldsymbol{\varphi}_k^{\mathrm{H}}\mathbf{y}_{\mathrm{p},m} = \sqrt{\tau^{cf}\rho_p}\, g_{mk} + \sqrt{\tau^{cf}\rho_p}\sum_{k'\neq k}^{K} g_{mk'}\boldsymbol{\varphi}_k^{\mathrm{H}}\boldsymbol{\varphi}_{k'} + \boldsymbol{\varphi}_k^{\mathrm{H}}\mathbf{w}_{\mathrm{p},m}. \quad (3)$$

Although $\breve{y}_{p,mk}$ may not serve as a sufficient statistic for estimating g_{mk} in the general case of arbitrary pilot sequences, it can still be used to derive suboptimal channel estimates. However, when the pilot sequences are designed such that any pair is either identical or mutually orthogonal, $\breve{y}_{p,mk}$ becomes a sufficient statistic, and the corresponding channel estimates based on it are statistically optimal.

In this special case, the minimum mean square error (MMSE) estimate of the channel coefficient g_{mk}, conditioned on the projected observation $\breve{y}_{p,mk}$, is given by:

$$\hat{g}_{mk} = \frac{\mathbb{E}\left\{\breve{y}^{*}_{p,mk} g_{mk}\right\}}{\mathbb{E}\left\{\left|\breve{y}_{p,mk}\right|^{2}\right\}} \breve{y}_{p,mk} = c_{mk} \breve{y}_{p,mk}, \tag{4}$$

where

$$c_{mk} = \frac{\sqrt{\tau^{cf} \rho_p}\, \beta_{mk}}{\tau^{cf} \rho_p \sum_{k'=1}^{K} \beta_{mk'} \left|\boldsymbol{\varphi}_k^{H} \boldsymbol{\varphi}_{k'}\right|^{2} + 1}. \tag{5}$$

2.4. Uplink data transmission

The received signal at the m^{th} AP is expressed by the following Eq. (6):

$$y_{u,m} = \sqrt{\rho_u} \sum_{k=1}^{K} g_{mk} \sqrt{\alpha_k} q_k + w_{u,m}, \tag{6}$$

where ρ_u represents the normalized uplink SNR, α_k represents the power control coefficient for the uplink data transmission of the k^{th} sensor, subject to the condition $0 < \alpha_k \leq 1$. This coefficient enables the system to adjust the transmission power of each sensor, thereby controlling the signal strength and minimizing interference. Let q_k denote the signal transmitted from the k^{th} sensor to the m^{th} AP, and let $w_{u,m}$ represent the noise vector at the m^{th} AP, which is assumed to follow a complex Gaussian distribution with zero mean and unit variance, describes the random interference factors in the transmission environment. To detect the signal q_k transmitted from the k^{th} sensor, the m^{th} AP multiplies the received signal $y_{u,m}$ by the conjugate of the channel estimate $\hat{g}_{mk}$. The result of this multiplication is forwarded to the CPU via a high-speed wired transmission link. The received signal at the CPU is expressed as:

$$r_{u,k} = \sum_{k'=1}^{K}\sum_{m=1}^{M}\sqrt{\rho_u \alpha_{k'}}\hat{g}_{mk}^{*} g_{mk'} q_{k'} + \sum_{m=1}^{M}\hat{g}_{mk}^{*} w_{u,m}. \quad (7)$$

The explicit expression for the achievable uplink data rate of the k^{th} sensor under power control is given as follows:

$$R = \log_2\left(1 + \frac{\rho_u \alpha_k \left(\sum_{m=1}^{M}\gamma_{mk}\right)^2}{\rho_u \sum_{k'\neq k}^{K}\alpha_{k'}\left(\sum_{m=1}^{M}\gamma_{mk}\frac{\beta_{mk'}}{\beta_{mk}}\right)^2 \left|\boldsymbol{\varphi}_k^H \boldsymbol{\varphi}_{k'}\right|^2 + \rho_u \sum_{k'=1}^{K}\alpha_{k'}\sum_{m=1}^{M}\gamma_{mk}\beta_{mk'} + \sum_{m=1}^{M}\gamma_{mk}}\right) \quad (8)$$

where $\boldsymbol{\varphi}_k$ denotes the pilot signal sequence transmitted by the k^{th} sensor to the APs to facilitate the channel estimation process, and

$$\gamma_{mk} = \frac{\tau^{cf}\rho_p \beta_{mk}^2}{\tau^{cf}\rho_p \sum_{k'=1}^{K}\beta_{mk'}\left|\boldsymbol{\varphi}_k^H \boldsymbol{\varphi}_{k'}\right|^2 + 1}. \quad (9)$$

The throughput of the k^{th} sensor during uplink data transmission is computed using the following expression:

$$T = \frac{1 - \frac{\tau^{cf}}{\tau^c}}{2} R. \quad (10)$$

In Eq. (10), the factor $\frac{1 - \frac{\tau^{cf}}{\tau^c}}{2}$ reflects the pilot overhead under the assumption that the coherence interval τc\tau_cτc is equally divided between uplink and downlink. Since the pilot transmission only occurs in the uplink phase, it occupies half of the total coherence interval. This modeling approach follows standard assumptions used in cell-free massive MIMO literature such as in [12], [13], and ensures a fair estimation of net throughput.

3. Throughput window-based power control

The TWC algorithm adjusts sensor power to maintain throughput within a desired range, ensuring energy efficiency while preserving communication quality. In this algorithm, sensors with throughput lower than the lower threshold increase their transmission power by a factor of η, whereas sensors with throughput exceeding the upper threshold reduce their transmission power by η. This process is iteratively

repeated until the throughput of all sensors falls within the range defined by the lower and upper thresholds or until a predefined number of iterations is reached. To achieve these objectives, the TWC algorithm is implemented through specific steps outlined in the algorithm flowchart in Fig. 2.

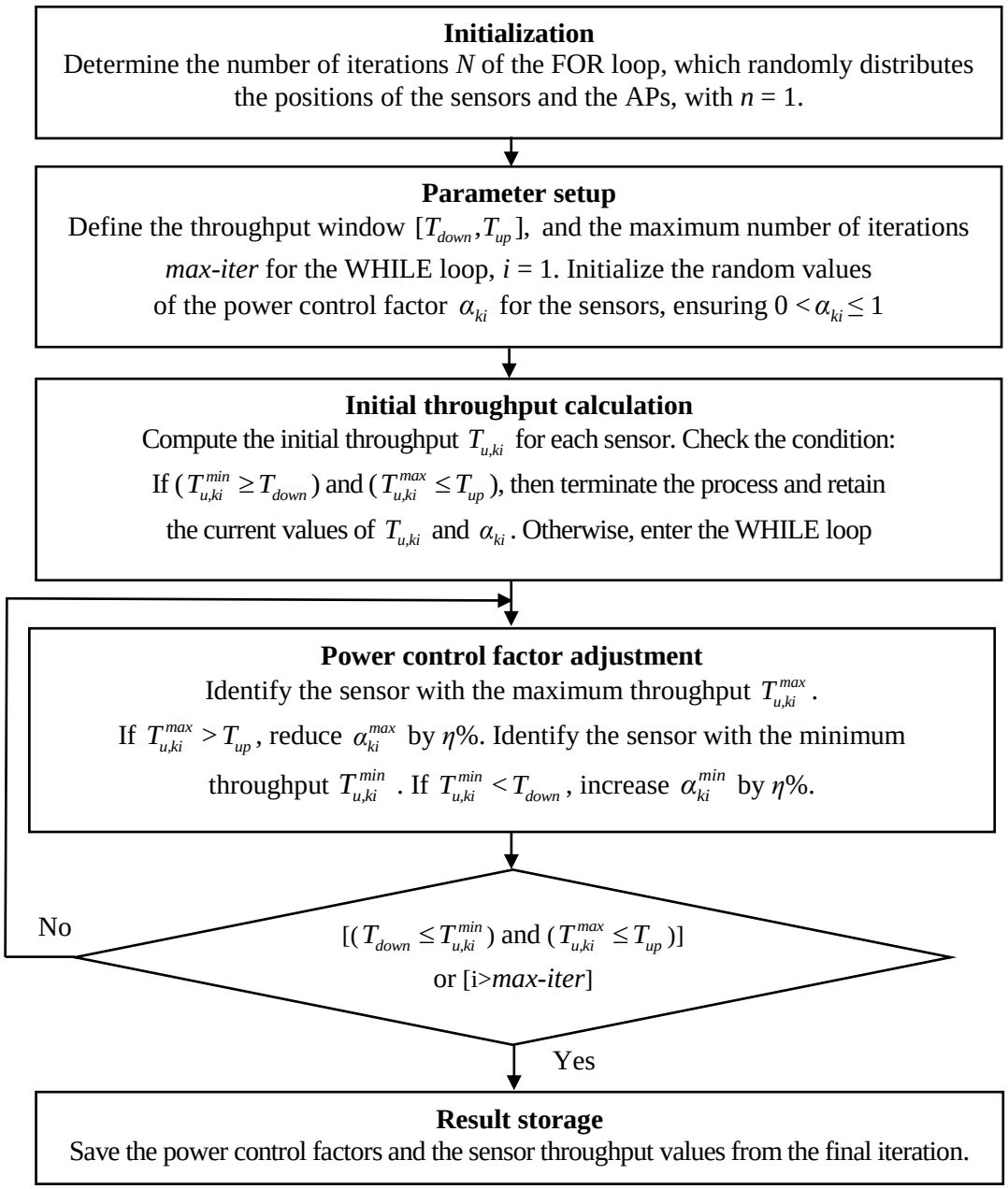

Fig. 2. Flowchart of the TWC algorithm.

4. Evaluation method

This section presents the methodology for investigating and evaluating the effectiveness of the proposed TWC power control algorithm, compared to the MMC algorithm and the No Power Control (NPC) scenario in the multi-connectivity WBAN model. The evaluation includes the simulation setup, system parameters, and performance metrics.

The performance of TWC, MMC, and NPC is evaluated based on sensor throughput and energy consumption. Sensor throughput is analyzed using the cumulative distribution function (CDF) which represents the probability that a sensor achieves a throughput lower than or equal to a given value. The CDF provides a comprehensive view of the throughput distribution in the system, enabling the assessment of power control algorithms. When comparing algorithms, a rightward shift in the CDF curve indicates higher average throughput, reflecting improved network performance. Conversely, a leftward shift in the CDF curve signifies reduced throughput, leading to lower transmission efficiency. Therefore, CDF analysis is a crucial tool for assessing throughput improvement in WBANs.

The energy consumption is evaluated using bar charts which illustrate the average energy expenditure of sensors under different algorithms. The bar charts facilitate the analysis of each method's effectiveness in minimizing energy consumption while maintaining stable connectivity. The combination of the CDF for throughput evaluation and bar charts for energy consumption analysis provides a comprehensive insight into the algorithm's performance in WBAN, aiding in the selection of the optimal power control strategy. The simulation setup parameters are detailed in Table 1.

Tab. 1. Simulation parameter setup

Parameter	**Value**
Frequency (f) [GHz]; Bandwidth (B) [MHz]	4.5; 10
Number of APs (M); Number of sensors (K)	4; 10
Height of AP (H_a), Height of sensor (H_c) [m]	2.5; from 0.5 to 1.5
Maximum transmission power of sensor (P_{max}) [mW]	1
Adjustment ratio of power control factor (η) [%]	1; 2; 5; 10
Lower throughput threshold (T_{down}) [Kbit/s]	10; 20; 30; 45
Upper throughput threshold (T_{up}) [Kbit/s]	20; 30; 45; 60
Room dimensions (length, width, height) [m]	10; 10; 3

The simulation considers 10 sensors and 4 APs uniformly deployed in a 100 m² indoor area, representing typical WBAN scenarios in hospital rooms or home-care environments. The use of multiple low-power APs follows the cell-free architecture, improving connectivity and interference management. Although the area is compact, it enables effective evaluation of power control under dense deployment. This setup reflects practical WBAN conditions while allowing clear performance analysis of the proposed algorithms.

5. Simulation results and discussion

5.1. Average throughput per sensor

The dashed line with triangular markers represents the case without power control (No Power Control - NPC). The simulation results in Fig. 3 indicate that under NPC, up to 85% of sensors achieve a throughput below the 30 Kbit/s threshold. This is primarily due to severe co-channel interference, which degrades the SNR and increases the bit error rate (BER), leading to a significant reduction in transmission efficiency.

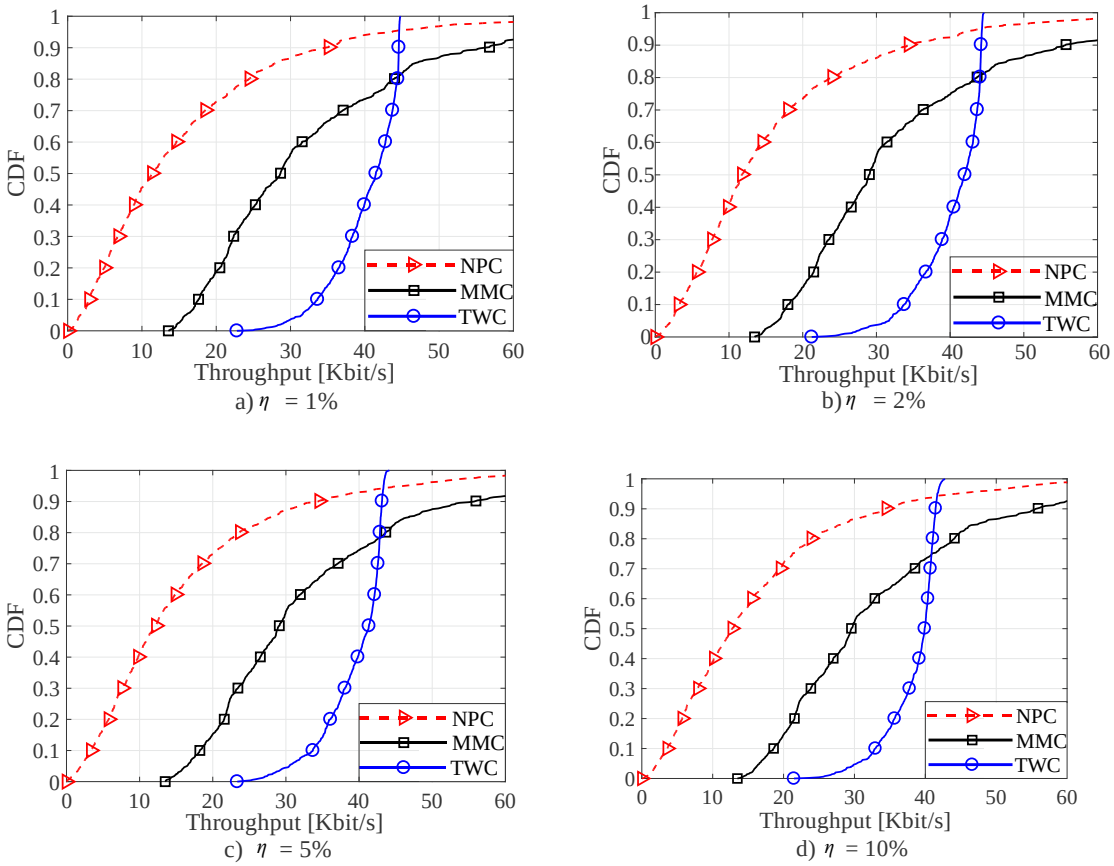

Fig. 3. Cumulative distribution of average throughput per sensor.

Sensors transmit at a fixed power level without an appropriate adjustment mechanism, leading to overlapping interference among signals. In particular, sensors located near the AP may transmit at excessively high power, causing unnecessary interference to neighboring sensors, while distant sensors may fail to transmit with sufficient power to overcome background noise and channel attenuation, resulting in a significant throughput reduction. Due to the lack of adaptation to channel conditions, sensors maintain a constant power level even under poor channel quality, which reduces bandwidth efficiency and creates an imbalance in network resource allocation. Consequently, the majority of sensors experience limited throughput, leading to a severe degradation in overall system performance.

The solid line with square markers represents the case where the MMC algorithm is applied. The simulation results in Fig. 3 show that 50% of sensors achieve a throughput below the 30 Kbit/s threshold, while the remaining 50% attain throughput above this level. The MMC algorithm adjusts the transmission power of each sensor to maximize the throughput of the lowest-performing sensor, thereby reducing the disparity in data transmission performance among sensors. However, since the algorithm prioritizes improving the performance of sensors with poor channel conditions, half of the sensors still experience a throughput limitation below 30 Kbit/s due to the effects of interference and channel attenuation. This outcome reflects the core principle of the MMC algorithm - enhancing the throughput of the weakest sensors but not necessarily optimizing the average throughput of the entire system.

The solid line with circular markers represents the case where the TWC algorithm is applied. This algorithm adjusts transmission power to maintain sensor throughput within the range of 30 Kbit/s to 45 Kbit/s. The simulation results in Fig. 3 show that most sensors achieve throughput within this range, with no sensor exceeding 45 Kbit/s. However, approximately 2% of sensors still experience throughput below 30 Kbit/s. This phenomenon, despite the TWC algorithm being designed to maintain throughput within the desired range, primarily stems from severe channel attenuation, high interference, and limitations in power adjustment capability. Some sensors located too far from the AP or obstructed by obstacles experience significant signal degradation, making even the maximum transmission power insufficient to compensate for channel losses under harsh conditions, preventing throughput from staying above 30 Kbit/s. These are inherent limitations that arise when sensor positions are randomly distributed and channel conditions exhibit significant heterogeneity. In the TWC algorithm, each sensor is allowed to adjust its transmit power to maintain the throughput within a predefined range $[T_{down}, T_{up}]$. However, if a sensor experiences severely degraded channel conditions (e.g., due to high path loss), even increasing the transmit power to its

maximum limit may not be sufficient to achieve the desired throughput. In such cases, the algorithm is constrained by the physical hardware limitations and can no longer increase the power to improve the link quality.

Observing charts (a), (b), (c) and (d) in Fig. 3 reveals that as η increases from 1% to 10%, the trends of NPC and the MMC algorithm remain unchanged, while the TWC algorithm also exhibits no significant fluctuations. This indicates that TWC operates stably, consistently maintaining the average throughput of each sensor within the predefined throughput window, regardless of variations in η.

5.2. Average throughput of sensors

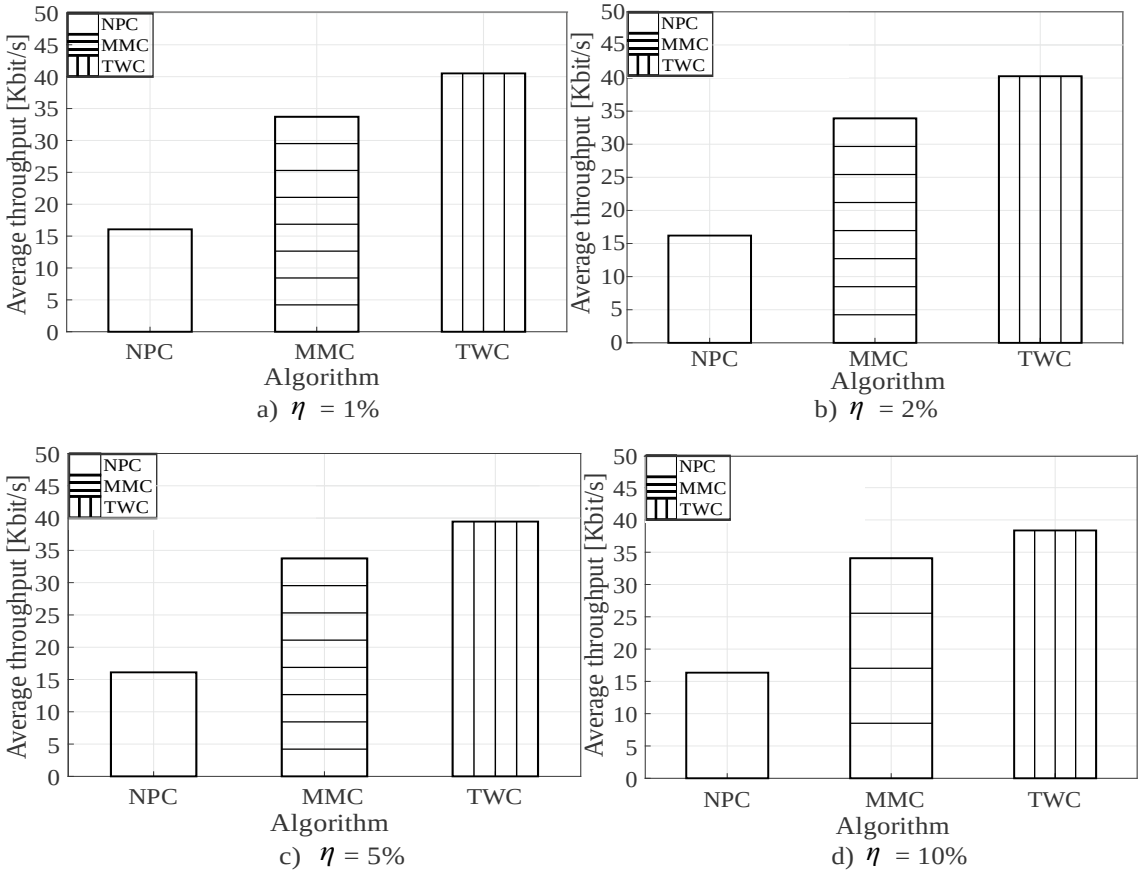

Fig. 4. Average throughput of all sensors.

The first column represents the NPC case. The simulation results in Fig. 4 show that NPC achieves the lowest average throughput, approximately 15 Kbit/s. This is primarily due to the lack of a transmission power optimization mechanism, which leads to high co-channel interference, thereby degrading data transmission performance, especially for sensors with poor channel conditions.

The second column represents the case where the MMC algorithm is applied. The simulation results in Fig. 4 show that the MMC algorithm achieves an average throughput of approximately 35 Kbit/s which is higher than NPC but still lower than the TWC algorithm.

The third column represents the case where the TWC algorithm is applied. The simulation results in Fig. 4 show that the TWC algorithm achieves superior performance, with an average throughput of 40 Kbit/s, which is 2.7 times higher than NPC and significantly outperforms the MMC algorithm.

Observing charts (a), (b), (c) and (d) in Fig. 4 reveals that as η increases from 1% to 10%, the trends of NPC and the MMC algorithm remain unchanged, while the TWC algorithm exhibits only minor fluctuations. This demonstrates that the TWC algorithm operates stably, consistently maintaining the average throughput of sensors within the defined throughput window, regardless of variations in η.

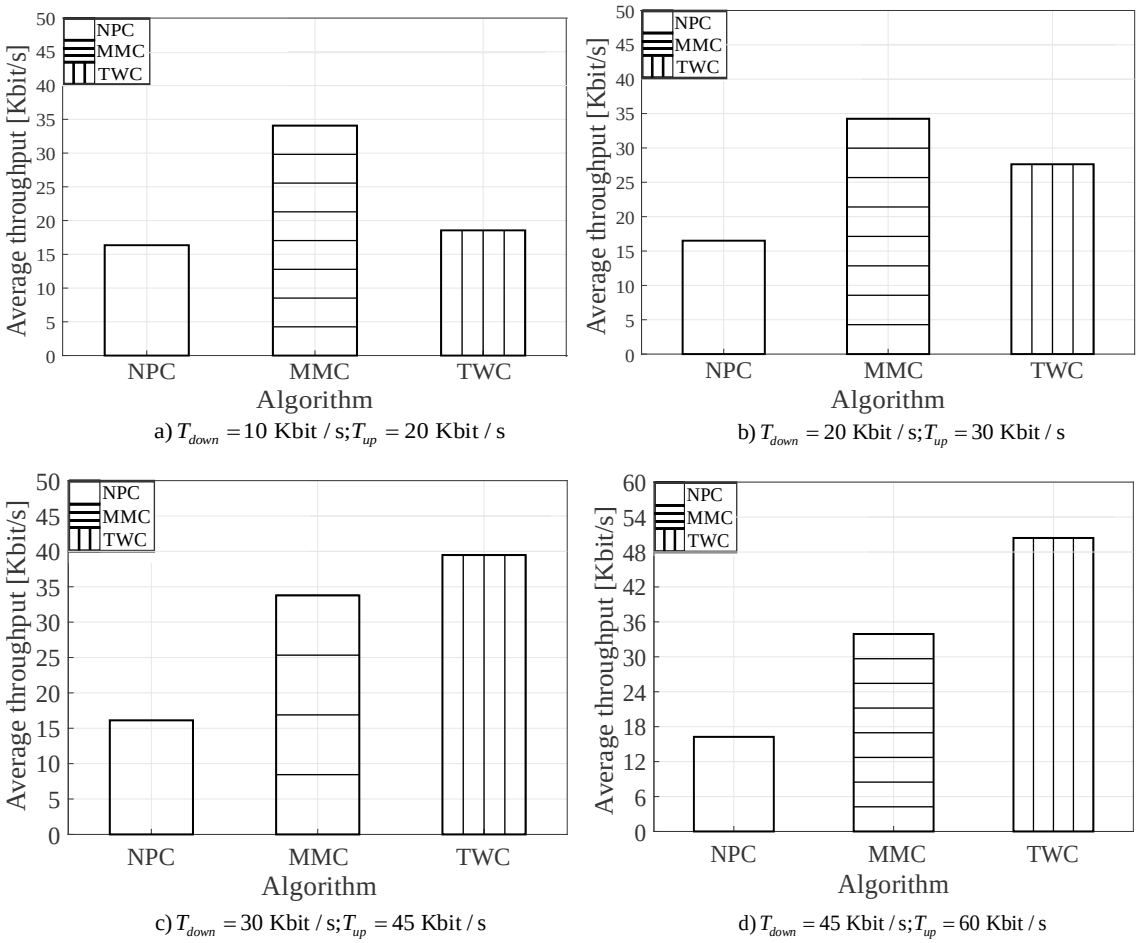

Fig. 5. Average throughput of all sensors with different throughput thresholds.

Simulation results in Fig. 5 (subplots (a) to (d)) show that the average throughput of the sensors under the TWC algorithm remains consistently within the target threshold range $[T_{down}; T_{up}]$, clearly demonstrating the algorithm's flexibility in accommodating different quality-of-service requirements. In contrast, the NPC and MMC schemes are not threshold-driven, resulting in throughput values that remain nearly constant regardless of changes in the threshold settings.

5.3. Average energy efficiency of sensors

In Fig. 6, the x-axis represents the index of each sensor from 1 to 10, along with an aggregate column indicating the average value (AVG). At each sensor position, three bars represent different cases: the first bar (without a pattern) corresponds to NPC, the second bar (horizontally striped) represents the MMC algorithm, and the third bar (vertically striped) denotes the TWC algorithm. Based on the simulation results in Fig. 6, several key observations can be made as follows:

- Across all sensors, the TWC bar consistently exhibits the greatest height compared to the other bars, with efficiency levels ranging from 115 Kbit/s/mW to 125 Kbit/s/mW and an average value of approximately 120 Kbit/s/mW. This indicates that the TWC algorithm utilizes energy most efficiently to enhance throughput.

- The MMC bar is consistently lower than the TWC bar, with efficiency levels fluctuating around 75 Kbit/s/mW. This indicates that MMC prioritizes increasing the transmission power for low-throughput sensors to ensure fairness rather than optimizing overall network efficiency. As a result, many sensors transmit at higher power levels than necessary, leading to increased energy consumption without significantly improving overall throughput.

- Due to the absence of a transmission power adjustment mechanism, sensors transmit signals at a fixed power level regardless of channel conditions. As a result, NPC achieves the lowest energy efficiency, with the NPC bar remaining below 20 Kbit/s/mW, indicating high energy consumption while yielding minimal throughput.

- Observing charts (a), (b), (c) and (d) in Fig. 6 reveals that as η increases from 1% to 10%, the trends of NPC and the MMC algorithm remain unchanged, while the TWC algorithm exhibits only minor fluctuations. This demonstrates that the TWC algorithm operates stably, consistently maintaining sensor energy efficiency at a higher level compared to NPC and MMC, regardless of variations in η.

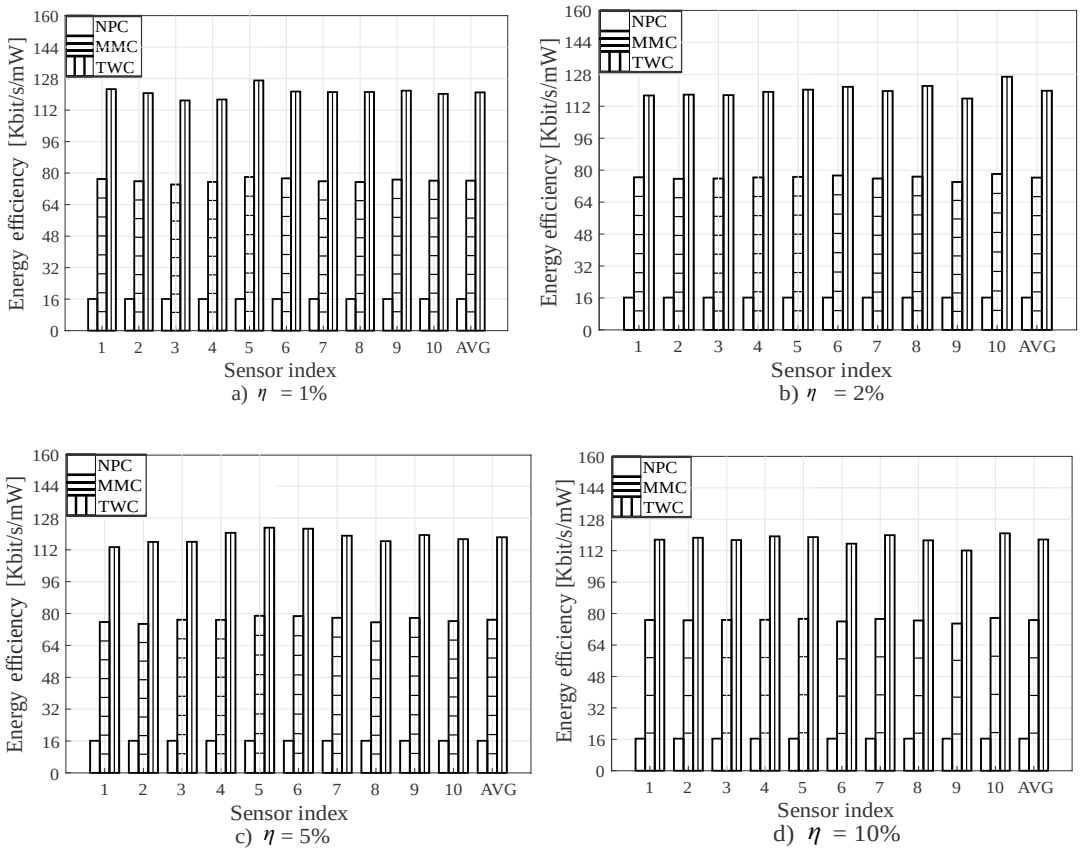

Fig. 6. Average energy efficiency of sensors.

5.4. Average power consumption of sensors

The simulation results in Fig. 7 show that, in the absence of power control, the average power consumption is the highest due to the lack of a transmission power optimization mechanism. Sensors always transmit at a fixed power level regardless of channel conditions, leading to severe energy wastage. Consequently, NPC exhibits higher average power consumption compared to the two power control algorithms, TWC and MMC.

The MMC algorithm exhibits lower average power consumption than NPC but remains higher than TWC. This algorithm adjusts transmission power based on a balancing criterion, aiming to enhance the throughput of the lowest-performing sensor in the system. This mechanism ensures that all sensors maintain an acceptable throughput level, rather than allowing some sensors to experience excessively low throughput. However, since MMC prioritizes improving the performance of weaker sensors, it may consume more power than TWC in certain scenarios.

The TWC algorithm achieves the lowest average power consumption. This is attributed to its power control mechanism which ensures that each sensor's throughput remains within a predefined threshold range. Specifically, if the throughput exceeds the upper threshold, the transmission power is reduced to conserve energy. Conversely, if the throughput falls below the lower threshold, the power is increased to maintain communication performance. As a result, TWC effectively balances energy consumption and data transmission efficiency, enabling energy savings while ensuring communication quality.

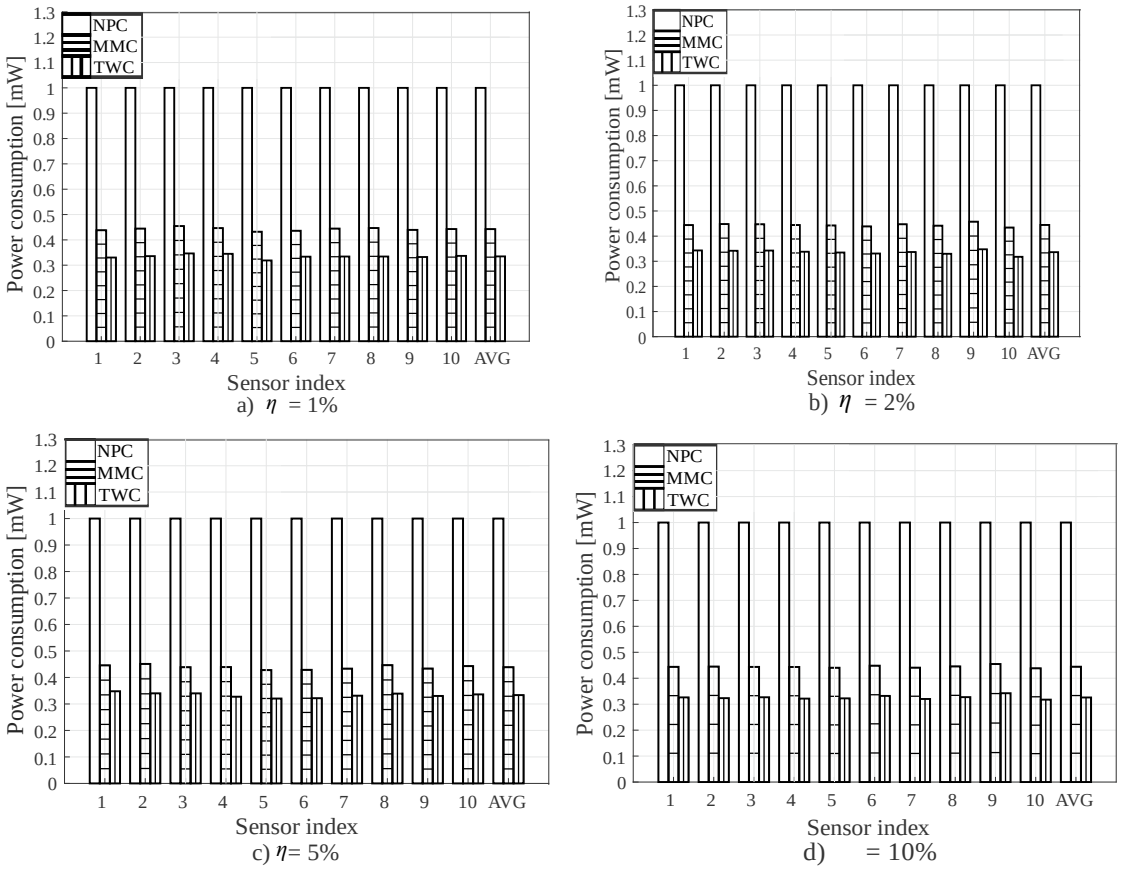

Fig. 7. Average power consumption of sensors.

Observing charts (a), (b), (c) and (d) in Fig. 7 reveals that as η increases from 1% to 10%, the trends of NPC and the MMC algorithm remain unchanged, while the trend of the TWC algorithm exhibits no significant fluctuations. This demonstrates that the TWC algorithm operates stably, consistently maintaining the average power

consumption of sensors at a lower level compared to NPC and MMC, regardless of variations in η.

6. Conclusion and future directions

Based on the simulation results, several key conclusions can be drawn. The TWC algorithm achieves the best performance by maintaining stable throughput within the target range, ensuring consistency, high reliability, and minimal variation among sensors. It also attains the highest energy efficiency by flexibly adapting to network conditions and effectively controlling transmission power to reduce energy waste.

In comparison, the MMC algorithm delivers moderate performance, as some sensors still fail to meet the desired throughput and consume more energy than TWC. Meanwhile, the NPC scheme performs the worst, with most sensors unable to reach the required throughput, resulting in severe co-channel interference, increased energy consumption, and significant degradation in overall system performance. The proposed TWC algorithm demonstrates strong potential for low-power WBAN applications such as remote health monitoring. Current limitations include simplified channel models, lack of mobility consideration, and absence of hardware validation. Future research will explore mobility-aware extensions, real-world deployment, and hybrid approaches that combine the strengths of TWC and MMC to balance throughput and energy efficiency. Expanding simulations to dense networks with interference and latency, and validating in IoT, 5G, and 6G scenarios will further enhance applicability in healthcare, industry, and sports.

References

[1] H. Taleb *et al*., "Wireless technologies, medical applications and future challenges in WBAN: A survey", *Wireless Networks*, Vol. 27, No. 8, pp. 5271-5295, Sep. 2021. DOI: 10.1007/s11276-021-02780-2

[2] M. Yaghoubi *et al*., "Wireless body area network (WBAN): A survey on architecture, technologies, energy consumption, and security challenges", *Journal of Sensor and Actuator Networks*, Vol. 11, No. 4, p. 67, Oct. 2022. DOI: 10.3390/jsan11040067

[3] L. Zhong *et al*., "Technological requirements and challenges in wireless body area networks for health monitoring: A comprehensive survey", *Sensors*, Vol. 22, No. 9, pp. 3-6, May 2022. DOI: 10.3390/s22093539

[4] M. Asam *et al*., "Challenges in wireless body area network", *International Journal of Advanced Computer Science and Applications*, Vol. 10, No. 11, Jan. 2019. DOI: 10.14569/IJACSA.2019.0101147

[5] M. J. Ali *et al.*, "Energy aware competitiveness power control in relay-assisted interference body networks", *5th International Workshop on Advances in ICT Infrastructure and Services*, 17-19 Jan. 2017. DOI: 10.48550/arXiv.1701.08295

[6] A. Moin *et al.*, "Adaptive body area networks using kinematics and biosignals", *IEEE Journal of Biomedical and Health Informatics*, Vol. 25, No. 3, pp. 623-633, March 2021. DOI: 10.1109/JBHI.2020.3003924

[7] Seemandhar Jain and Prarthi Jain, "An energy efficient health monitoring approach with wireless body area networks", *ACM Transactions on Computing for Healthcare (HEALTH)*, Vol. 3, Iss. 3, Apr. 2022. DOI: 10.1145/3501773

[8] W. Gao *et al.*, "Transmission power control for IEEE 802.15.6 body area networks", *ETRI Journal*, Vol. 36, No. 2, pp. 313-316, Apr. 2014. DOI: 10.4218/etrij.14.0213.0220

[9] L. Wang *et al.*, "Joint optimization of power control and time slot allocation for wireless body area networks via deep reinforcement learning", *Wireless Networks*, Vol. 26, No. 6, pp. 4507-4516, May 2020. DOI: 10.1007/s11276-020-02353-9

[10] B. Q. Bao *et al.*, "Joint throughput equalization power control and cell-free model for enhancing performance of WBANs", *Wireless Personal Communications*, Vol. 139, pp. 921-946, Nov. 2024. DOI: 10.1007/s11277-024-11647-6

[11] H. Q. Ngo *et al.*, "Cell-free massive MIMO versus small cells", in *IEEE Transactions on Wireless Communications*, Vol. 16, No. 3, pp. 1834-1850, Mar. 2017. DOI: 10.1109/TWC.2017.2655515

[12] H. Q. Ngo *et al.*, "Energy and spectral efficiency of very large multiuser MIMO systems", *IEEE Transactions on Communications*, Vol. 61, No. 4, pp. 1436-1449, Apr. 2013. DOI: 10.1109/TCOMM.2013.020413.110848

[13] T. L. Marzetta *et al.*, *Fundamentals of Massive MIMO*, Cambridge University Press, 2016. DOI: 10.1017/CBO9781316799895

PHÁT TRIỂN THUẬT TOÁN ĐIỀU KHIỂN CÔNG SUẤT DỰA TRÊN CỬA SỔ THÔNG LƯỢNG CHO MẠNG VÔ TUYẾN QUANH CƠ THỂ

Bùi Tiến Anh[1], Đỗ Thành Quân[2], Phùng Quang Quân[3], Phạm Thanh Hiệp[1]

[1]*Khoa Vô tuyến điện tử, Trường Đại học Kỹ thuật Lê Quý Đôn*

[2]*Khoa Chỉ huy Tham mưu kỹ thuật, Trường Đại học Kỹ thuật Lê Quý Đôn*

[3]*Trung tâm Hợp tác quốc tế Khoa học công nghệ Việt - Nhật, Trường Đại học Kỹ thuật Lê Quý Đôn*

Tóm tắt: Các cảm biến trong mạng vô tuyến quanh cơ thể (*Wireless Body Area Networks - WBAN*) yêu cầu tiêu thụ năng lượng thấp để đảm bảo hoạt động liên tục trong thời gian dài, đồng thời duy trì khả năng truyền dữ liệu chính xác và ổn định. Bài báo đề xuất một thuật toán điều khiển công suất mới nhằm tiết kiệm năng lượng cho cảm biến trong WBAN. Thuật toán "điều khiển công suất dựa trên cửa sổ thông lượng" (*Throughput Window-based Power Control - TWC*) được đề xuất nhằm đảm bảo thông lượng cho cảm biến nằm trong một khoảng giá trị nhất định, phù hợp với yêu cầu hệ thống. Kết quả mô phỏng cho thấy thuật toán TWC không chỉ giúp giảm đáng kể mức tiêu thụ năng lượng mà còn duy trì hiệu suất truyền tin ổn định với độ tin cậy cao trong điều kiện truyền dẫn đặc thù của WBAN. Cụ thể, thuật toán TWC đạt hiệu quả năng lượng trung bình cao nhất, cao hơn 1,5 lần so với thuật toán điều khiển công suất tối đa hóa mức tối thiểu (MMC) và cao hơn 7,5 lần so với trường hợp không điều khiển công suất (NPC). Ngoài ra, TWC còn cho mức tiêu thụ năng lượng trung bình thấp nhất, chỉ bằng 0,75 lần so với MMC và 0,3 lần so với NPC. So với thuật toán MMC và trường hợp NPC, TWC thể hiện khả năng tiết kiệm năng lượng vượt trội trong khi vẫn đảm bảo chất lượng dịch vụ. Những kết quả này góp phần thúc đẩy phát triển các mô hình WBAN tự chủ về năng lượng, đáp ứng yêu cầu của các ứng dụng giám sát sức khỏe tiên tiến.

Từ khóa: *Mạng vô tuyến quanh cơ thể; điều khiển công suất; tiết kiệm năng lượng; hiệu suất truyền tin.*

Received: 07/03/2025; Revised after review: 14/04/2025; Accepted for publication: 23/05/2025

❑